

RECENT DEVELOPMENTS OF THE 3D FIBER PROBE

Ulrich Neuschaefer-Rube¹, Holger Bremer², Benjamin Hopp³, Ralf Christoph³

1 Physikalisch-Technische Bundesanstalt, Bundesallee 100, 38116 Braunschweig, Germany,
ulrich.neuschaefer-rube@ptb.de

2 Physikalisch-Technische Bundesanstalt, 3 Werth Messtechnik GmbH

Abstract:

The fiber probe is well known in micro-coordinate metrology. The 2D version has been used for many years to measure injector nozzles, turbine blade cooling holes, and a variety of other small, tight tolerance features. A development of this probe, the 3D fiber probe, has been commercially available for some time.

In a cooperation project, PTB and Werth Messtechnik have continued investigations on this microprobe. This paper reports on the recent achievements. Very small stylus tips with diameters down to 25 μm with isotropic stiffness and novel probe designs are now possible. Dual-sphere and L-shaped styli have opened new applications for holes with large aspect ratios and recessed features. Scanning tests have resulted in form deviations below 0.4 μm .

This paper explains the operating principle, reports on test results and describes some of the applications.

Keywords: Coordinate metrology, microprobe, tactile-optical probe, WFP 3D, 3D fiber probe

1. INTRODUCTION

The fiber probe combines tactile probing with the accurate optical measurement of the probe tip position [1]. In comparison to other tactile microprobes [2] the measurement signal is not transferred mechanically by the probe shaft. Therefore, the probing forces can be very low (1 μN to 100 μN) and stylus tips are available with much smaller diameters (down to 25 μm). The 2D version of this probe has been used for many years with Werth Coordinate Measuring Machines. It has been frequently combined with other sensors in a multisensor approach for various applications. Several concepts have been developed in an attempt to accomplish 3D fiber probes. For example, the tip deflection in the third dimension was determined by a second optic, stereo techniques, or the evaluation of speckle patterns created at different focal lengths by the refraction of a laser [3, 4].

For some time a 3D fiber probe has been commercially available which determines the tip deflection in line with the optical axis by an optical distance sensor. The main advantages compared to the other 3D-setups are minimal hardware, robustness and small drift effects due to the basic principle.

2. PRINCIPLE OF OPERATION

Similar to the 2D fiber probe, the 3D fiber probe (see Figure 1) combines tactile probing with accurate optical measurement of the tip position. The microprobe consists of an optical glass fiber acting as the stylus with a small

spherical tip attached to the end. The tip is mounted in the focal plane of the imaging system of an optical coordinate measuring machine (CMM). It is mirror-coated on the lower hemisphere for reflectivity. The fiber is fixed on an optical CMM by a three curved prong leaf spring with low stiffness. This arrangement ensures the flexibility of the probe in all axes.

The determination of the tip position in the horizontal axes to the optics (x- and y-directions) is similar to the 2D probe: The image of the illuminated stylus tip is located in the camera image of the optical CMM by correlation techniques.

The stylus position parallel to the optical axis is determined by a laser distance sensor which measures the height of the upper end of the fiber (see Figure 1: top). This sensor is based on the Foucault laser principle [5].

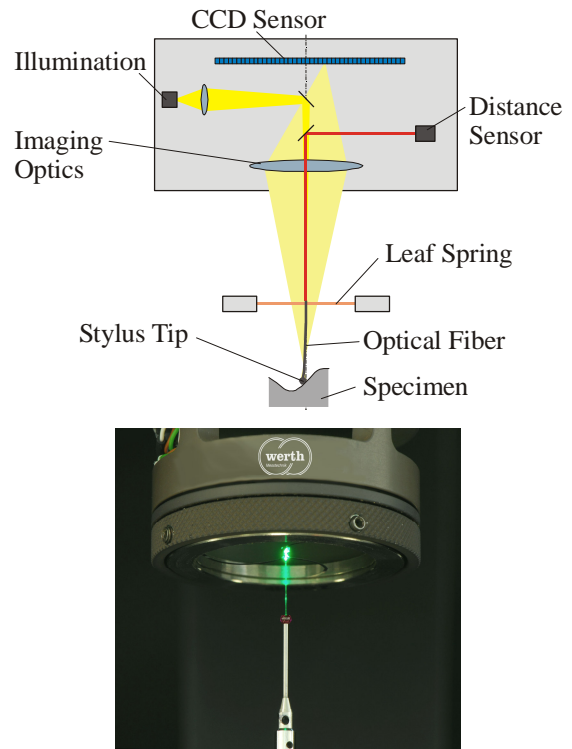


Fig. 1: 3D fiber probe: Top: Principle of operation, Bottom: Probe measuring a ruby sphere ($\varnothing 2$ mm)

3. ADVANCED PROBE DESIGNS

3.1 Improved spring design

Fiber probes are light and very elastic. Even small probing forces ($\ll 1$ mN) can result in large displacements

of the stylus tip. This is especially the case for tips with smaller diameters and consequently smaller shaft diameters. To create probes with nearly isotropic compliance, special attention has been paid to the spring design by finite element method (FEM) calculations. The parameter describing this isotropy is the ratio between the compliance in the xy-plane and the compliance in the z-direction.

Figure 2 shows the standard spring design and an improved version for probes with smaller stylus tips.

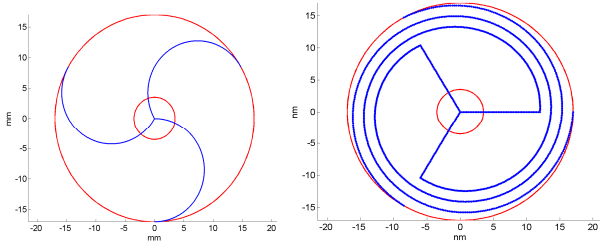


Fig. 2: Designs of the leaf spring: Left: Standard design, Right: Improved design.

The spring design is depicted in blue. The outer red circle symbolizes the edge of the mounting. The inner circle shows the boundary of the camera's field of view.

The standard design consists of three curved prongs and allows compliance ratios down to 1.4:1 for standard probes (tip diameter: approx. 250 μm). For smaller tip diameters and consequently thinner styli, the compliance ratio becomes gradually worse and the compliance becomes bigger. This results in smaller probing forces. If the probing forces become too small, significant adhesion effects between the tip and workpiece will occur.

The new design is intended to increase the probing forces while maintaining a compliance ratio of 1:1. Comparisons between the standard and the improved design show that the probing force has been doubled while retaining the same compliance ratio. With additional minor modifications, compliance ratios of 1:1 can be achieved for probes with tip diameters of less than 100 μm .

3.2 Dual-sphere styli

In addition to the standard design, styli with two spheres are also available. With the standard design, shadowing effects occur if steep flanks are measured. These effects will be eliminated with dual-sphere styli.

Both spheres are arranged on the shaft with one affixed below the other. During measurements with a single sphere probe (section 2), the sphere is deflected with the workpiece and its deflected position is monitored by the optics. With the dual-sphere probe, the lower sphere is deflected with the workpiece while the deflected position of the upper sphere is monitored. Thus, the potential for the optics to pick up the reflection of the sphere on shiny surfaces rather than the actual sphere is eliminated. The displacement ratio between both spheres must be calibrated one time prior to use.

The most simple design (see Figure 3) consists of a stylus with both spheres arranged vertically with one above the other. The distance between both spheres can be up to a few millimeters. This allows measurements of boreholes without

obstructions of the sphere by the sidewalls of the borehole. The diameter of the probing tip can also be reduced without affecting the visibility of the upper sphere and therefore without reducing the measurement accuracy by this optical effect. Larger distances between the two spheres lead to larger measurement deviations due to the smaller displacement of the upper sphere. Therefore, the distance between the spheres should be as small as possible depending on the application.

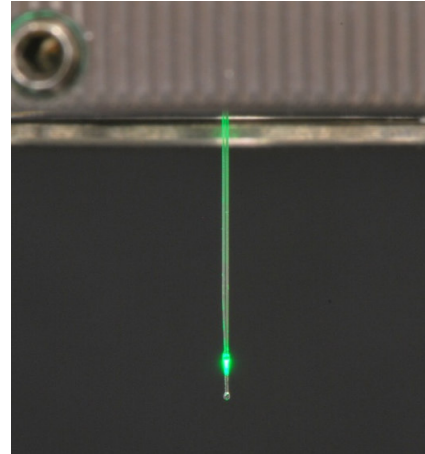


Fig. 3: Dual-sphere stylus.

3.3 L shaped styli

L shaped styli are a more advanced design of dual-sphere styli. These styli are constructed of a single fiber with two spheres that is bent below the upper sphere (see Figure 4). With this design, undercuts can be measured. The bend angle can be constructed to fit the measurement task.

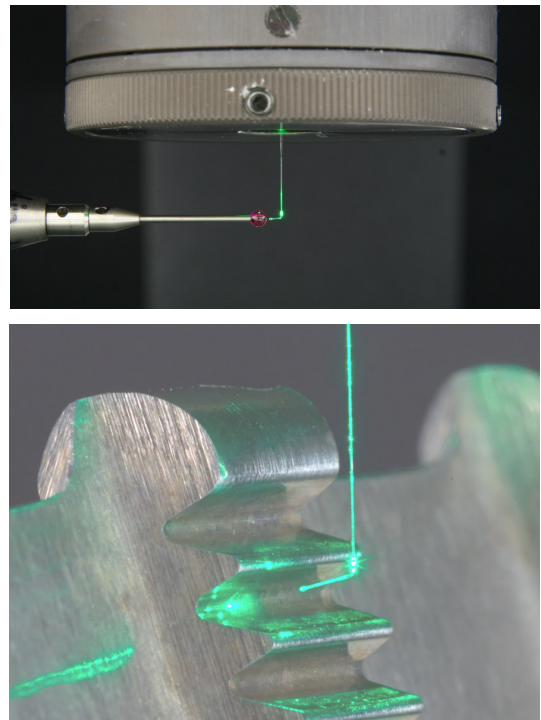


Fig. 4: L-shaped styli: Top: Stylus with a bend angle of 95° probing a ruby sphere, Bottom: Stylus with a bend angle of 115° probing a broach.

4. TEST RESULTS

Probing tests according to ISO 10360-5 were carried out with a Werth VideoCheck UA CMM equipped with a standard 3D fiber probe (tip diameter: 250 μm). Measurements of 25 points on a sphere (diameter: 10 mm) resulted in probing errors below 200 nm (P_F) (see Figure 5) and 100 nm (P_S).

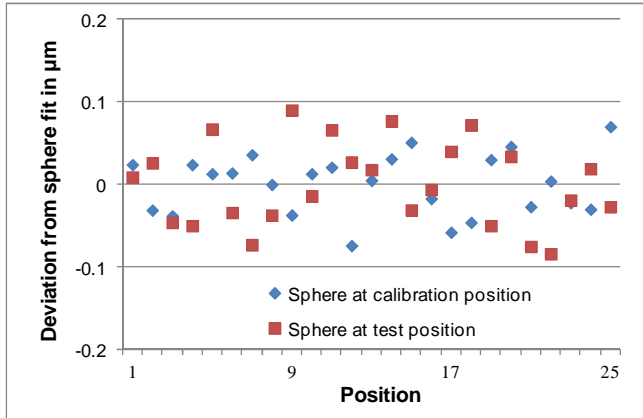


Fig. 5: Results of two probing tests according to ISO 10360-5.

Scanning probing errors THN according to ISO 10360-4 below 400 nm were achieved scanning a sphere (Figure 6). For this test, a probe with a tip diameter of 247 μm was used to scan a ruby sphere (diameter: 2.0004 mm).

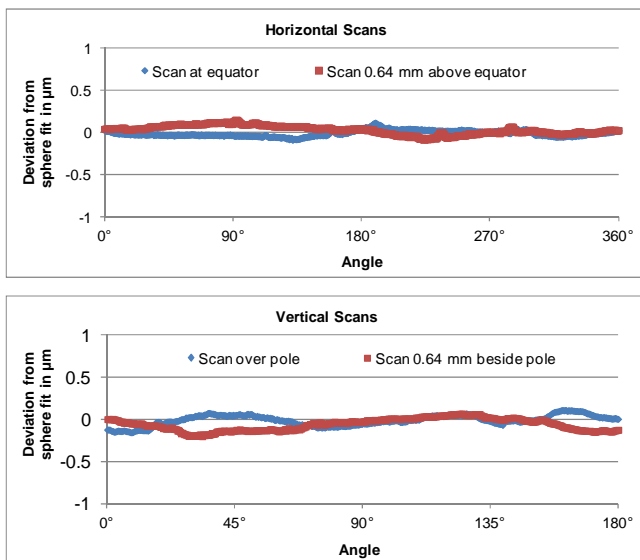


Fig. 6: Results of a scanning test according to ISO 10360-5: Deviation of the scanned points from the fitted sphere.

Figure 7 depicts the results of an extended probing test of a dual-sphere probe according to ISO 10360-5 on a ruby sphere (diameter: 2.0003 mm). Radial deviations from the sphere with the x- and y-position are shown as the tip center position for each point. The diameter of the tip was 254 μm and the upper sphere was 1.53 mm above the tip sphere. The ratio between the displacements of the upper sphere and the lower tip sphere was approximately 1:1.15.

The measurement of 25 points was repeated 10 times. Between the measurements the point grid was rotated by 36 $^\circ$.

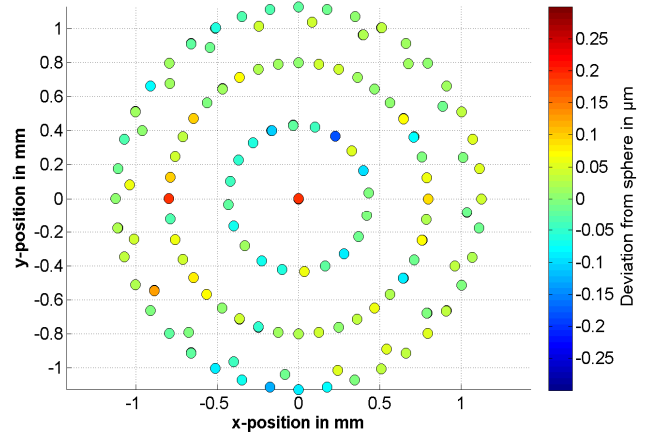


Fig. 7: Results of an extended probing test of a dual-sphere stylus.

The probing errors determined from the 10 data sets are $P_S = 0.230 \mu\text{m} \pm 0.022 \mu\text{m}$ and $P_F = 0.289 \mu\text{m} \pm 0.076 \mu\text{m}$. Scanning tests with the same dual-sphere stylus resulted in deviations similar to Figure 6.

5. APPLICATION EXAMPLES

5.1 Silicon standard

A standard made of silicon (see Figure 8) was measured with a standard 3D probe. The dimensions of the standard were 3 mm x 3 mm x 1 mm. The standard [6] was manufactured by anisotropic etching.

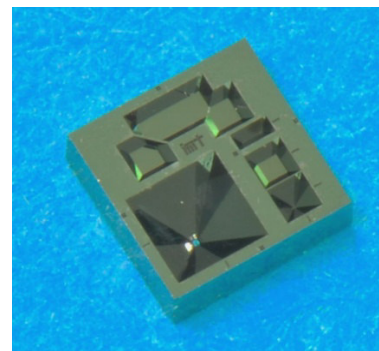


Fig. 8: Measured silicon standard (dimensions: 3 mm x 3 mm x 1 mm).

With the 3D fiber probe (tip diameter: 249 μm) the inverted pyramid shown below left in Figure 8 was scanned with a scanning speed of approximately 20 $\mu\text{m/s}$. The measured point cloud was fitted to the four planes of the pyramid. The deviations are shown in Figure 9.

Most of the deviations are smaller than 1 μm . There are a few larger deviations caused by particles. Additionally, there are larger deviations on the left surface where the tip was pushed in contrast to the right surface where it was pulled across the surface during the scan.

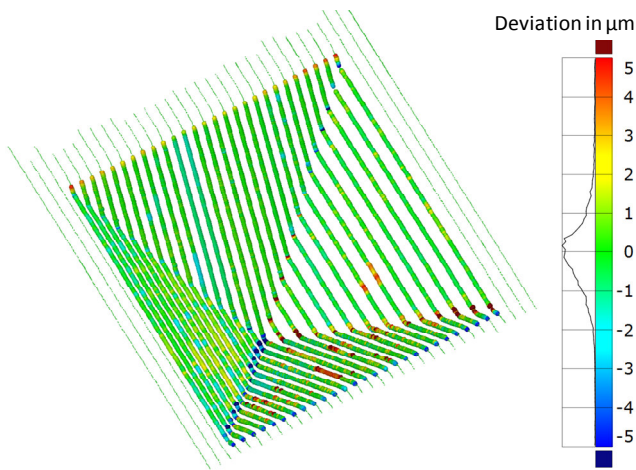


Fig. 9: Measurement results on a silicon standard.

As a result of the orientation of the crystal planes and the etching process, the nominal angle between opposing surfaces of the inverted pyramid was 70.52° . The measured angles between the respective fitted planes were 70.75° and 70.83° .

5.2 Thread gauge

An M2.6 thread gauge (Figure 10) was measured with a 3D fiber probe with an L-shaped stylus. The tip diameter was $120\ \mu\text{m}$. The results are shown in Figure 11.

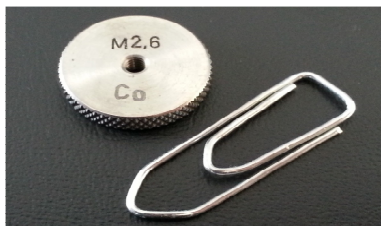


Fig. 10: Measured M2.6 thread gauge.

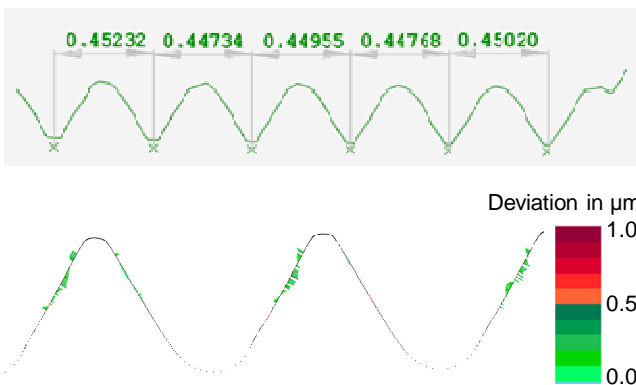


Fig. 11: Measurement results on an M2.6 thread gauge: Top: Thread pitch, Bottom: Tooth profile deviation.

The nominal value of the thread pitch was $0.45\ \text{mm}$. As shown in Figure 11, top, this value was very close to the measured pitch values.

In the bottom part of Figure 11 the tooth profile deviation is depicted. The deviations of the measured points from the

fitted lines on the respective flanks are displayed. All deviations were smaller than $0.5\ \mu\text{m}$.

6. CONCLUSIONS AND OUTLOOK

The 3D fiber probe was successfully tested to prove low measuring uncertainty. Probing tests according to ISO 10360 resulted in probing errors (P_F and P_S) of less than $200\ \text{nm}$ and scanning errors (THN) of less than $400\ \text{nm}$.

Unique advanced styli designs such as the dual-sphere and the L-shaped styli to broaden the application spectrum of the probe were presented and also successfully tested. Probing errors below $300\ \text{nm}$ were achieved.

Two applications examples demonstrated the versatility of the probe.

Additional investigations will be focused on very small styli with tip diameters down to $10\ \mu\text{m}$, on increased stiffness and on more complicated styli designs such as T and star configurations. Another emphasis will be the additional improvement of the accuracy.

ACKNOWLEDGEMENTS

This work is supported by the Federal Ministry of Economic Affairs and Energy (research program “MNPQ”, Az 05/12). The authors thank the ministry for funding this project.

REFERENCES

- [1] H. Schwenke, Ch. Weisskirch, and H. Kunzmann, “Opto-Tactile Sensor for 2D and 3D Measurement of small structures of Coordinate-Measuring Machines”, *Technisches Messen* 66(12), pp. 485-489 (1999).
- [2] A. Weckenmann, T. Estler, G. Peggs, G., and D. McMurtry, “Probing Systems in Dimensional Metrology, STC P”, *CIRP Annals*, 51(2), pp. 657 (2004).
- [3] U. Neuschaefer-Rube, M. Wissmann, “Tactile-optical 3D sensor applying image processing”, *Proc. SPIE* 7239, pp. 72390G-1 - 72290G-10 (2007).
- [4] R. Tutsch, M. Andräs, U. Neuschaefer-Rube, M. Petz, T. Wiedenhöfer, M. Wissmann, “Tactile-optical microprobes for three dimensional measurements of microparts”, *Proc. 10th ISMQC*, pp. E2-032-1 - E2-032-4 (2010).
- [5] R. Christoph, H.-J. Neumann, “Multisensor Coordinate Metrology”, Verlag Moderne Industrie München, Germany, 2007, ISBN 978-3-937889-66-5.
- [6] T. Krahl, F. Horn, S. Patzelt, C. Schrader, M. Schulze, L. Shaw, A. Tausendfreund, B. Viering, “Vergleich von Messverfahren zur Geometriebestimmung in der Mikrotechnik”, in: A. Weckenmann, “Neue Strategien der Mess- und Prüftechnik für die Produktion von Mikrosystemen und Nanostrukturen”, *final report of DFG priority program 1159*, Shaker Verlag, Aachen, Germany, pp. 234 - 249, 2011, ISBN 978-3-86247-156-0.